Hindawi
Advances in Civil Engineering
Volume 2023, Article ID 5119602, 7 pages
https://doi.org/10.1155/2023/5119602

Research Article

Determination of the Caving Zone and Fracture Zone Heights by Using the LK-Means Algorithm

Ze Zhou [1], Juncai Cao [2], Long Lai [3], Jinlian Zhou [4], and Mengtang Xu [1]

[1] *Institute of Mining Engineering, Guizhou Institute of Technology, Guiyang, China*
[2] *Guizhou Energy Co., Ltd., Guiyang, China*
[3] *Guizhou Energy Administration, Guiyang, China*
[4] *Huopu Coal Mine, Guizhou Pangjiang Refined Coal Co., Ltd., Guiyang, China*

Correspondence should be addressed to Ze Zhou; 1393493559@qq.com

Received 30 May 2023; Revised 22 September 2023; Accepted 1 November 2023; Published 11 December 2023

Academic Editor: Manoj Khandelwal

The caving zone and fracture zone frequently appear after coal excavation. However, the caving zone and fracture zone can hardly be obtained with an empirical equation. Therefore, identifying a proper method to determine the caving zone and fracture zone is critically important to engineering practice. In this paper, Universal Distinct Element Code numerical simulations were conducted. Furthermore, the LK-means algorithm was used to determine the caving zone and fracture zone heights. To verify the validity of the proposed method, two engineering case studies were used. It could be found that the height calculated by the proposed method agrees well with that determined in engineering tests. Hence, the proposed method can be used in engineering practice.

1. Introduction

After coal is excavated, the rock mass above the goaf can generally be classified into three zones [1, 2], which is the basis of coal excavation design [3, 4]. Based on the ground pressure and in situ tests, the upper rock mass of the goaf can be divided into three zones [5, 6]: the caving zone, fracture zone, and curve subsidence zone.

Due to the importance of these three zones in coal excavation design, gas drainage and ground building structures, the study of the three zones has remained a hot topic. Fu et al. [7] studied the caving zone height in the Shangwan Coal Mine by using ANSYS software. Moreover, the caving zone height in the Shangwan Coal Mine was analyzed. Through the analysis of numerical simulation results and in situ test data, it could be found that the caving zone height increases with increasing length of the working face and working face height, while the influence of the working face was less notable, and an empirical equation for calculating the caving zone in the Shangwan Coal Mine was proposed. Song et al. [8] found that the pressure on the support remarkably increases with increasing working face length and concluded that the caving zone increases with increasing working face length; however, in their study, no method for calculating the caving zone height was proposed. Teng et al. [9] found that the coal location greatly influences the fracture zone height and caving zone height. This conclusion is important for coal excavation design. Therefore, coal excavation location selection is critical. Xu et al. [10], Yi et al. [11], and Xu et al. [12] conducted engineering experiments and concluded that the primary key stratum imposes a notable influence on the caving zone height; hence, the primary key stratum location should be considered in estimating the caving zone height, and these results were also verified in other studies. Many other researchers have measured the three-zone height [13–21]; however, they mainly focused on the measurement of the caving zone height and fracture zone height in the field, which is a time-consuming and noneconomical process. Until now, no method has been determined for estimating the height of the three zones. Therefore, proposing a method for estimating the caving zone height and fracture zone height is critical for engineering practice.

To resolve this problem, the Universal Distinct Element Code (UDEC) numerical simulation method and the LK-means algorithm were combined to determine the caving zone height and fracture zone height. UDEC numerical simulations were conducted first. Subsequently, the displacement magnitude was exported by using FISH language. Via the use of the LK-means algorithm, the caving zone and fracture zone were determined, and the caving zone height and fracture zone height were then determined. To verify the validity of the proposed method, two numerical simulation examples were given, and the numerical simulation results were compared to in situ test data. The difference between the calculation results and the in situ test data is small. The proposed method is valid and can be used to calculate the heights of the caving zone and fracture zone.

2. Determination of the Caving Zone and Fracture Zone Heights

In this paper, the upper rock mass zone of the goaf was classified into a caving zone and a fracture zone based on the displacement of the upper rock mass. To implement the process, the LK-means algorithm was used, and the classification process is explained below.

2.1. LK-Means Algorithm. The LK-means algorithm is a combination of the XK-means clustering algorithm, Levy flying algorithm, and *K*-means algorithm [22].

The *K*-means clustering algorithm attempts to divide n groups of data into k classes, and each data point belongs to the nearest cluster of center points. For example, for a set of n groups of data $(x_1, x_2, x_3, \ldots\ldots, x_n)$, this set of data is d-dimensional. With the use of the *K*-means clustering algorithm, these data are divided into k $(k \leq n)$ sets $(S = S_1, S_2, S_3, \ldots\ldots S_k)$ to minimize the variance, which can be described as follows:

$$\underset{s}{\operatorname{argmin}} \sum_{i=1}^{k} \sum_{x \in S_i} ||x - u_i||^2 = \underset{s}{\operatorname{argmin}} |S_i| \operatorname{Var}(S_i), \tag{1}$$

where u_i is the mean value of the points in S_i. In the clustering process, the above is equivalent to minimizing the squared deviation of points in the same cluster.

$$\operatorname{argmin} \sum_{i=1}^{k} \left(\frac{1}{2|S_i|} \sum_{x,y \in S_i} ||x - y||^2 \right). \tag{2}$$

It can be deduced as follows:

$$\sum_{x,y \in S_i} ||x - y||^2 = \sum_{x \neq y \in S_i} (x - u_i)^{\mathrm{T}} (u_i - y). \tag{3}$$

However, the *K*-means algorithm can easily converge at local optima. To solve this problem, the XK-means clustering algorithm was proposed. In this algorithm, a random vector θ_j is added to the clustering centroid of the *K*-means algorithm.

$$D_j^* = D_j + \theta_j, \tag{4}$$

where θ_j is a random search vector, which can be determined as follows:

$$\theta_j = \operatorname{rand}(a_i, b_i) \times \operatorname{randsign}(i), i = 1, 2, \ldots, D, \tag{5}$$

where $\operatorname{rand}(a_i, b_i)$ is a random number between a_i and b_i. The relationship between a_i and b_i can be expressed as follows:

$$a_i = \beta b_i, \tag{6}$$

where β is a coefficient with a range of [0, 1]. Before the next iteration, the value of b_i can be expressed as follows:

$$b_i^* = \alpha b_i, \tag{7}$$

where α is a constant value, which occurs within the range of [0, 1).

However, based on previous studies, the XK-means algorithm cannot prevent convergence at local optimal values. Hence, a new clustering algorithm, namely, the LK-means algorithm, was proposed by Dasgupta et al. [23]. This algorithm is inspired by the XK-means algorithm, Levy flying algorithm, and *K*-means algorithm.

In the LK-means algorithm, the Levy flight path increases the diversity of random search vectors, and Levy flight strategies can be used to generate the new search vector, which can be expressed as follows:

$$\theta_j = \operatorname{rand}(a_i, b_i) \times \mu \operatorname{sign}\left[\operatorname{rand} - \frac{1}{2}\right] \otimes \text{Levy}, i = 1, 2, 3, \ldots\ldots, D, \tag{8}$$

where μ is a random number within the range of [0, 1], and $\operatorname{sign}[\operatorname{rand} - \frac{1}{2}]$ is the direction of the vector, which has three values: 0, 1, and −1.

In the exploration process, the number of iteration steps increases, which can be expressed as follows [24]:

$$\text{Levy} \sim u = t^{-\lambda}, 1 < \lambda \leq 3. \tag{9}$$

The Levy flight strategy exhibits both large and small steps in the search process. To imitate a lambda stable distribution by a random behavior similar to that of Levy flights, Mantegna's algorithm was proposed, which can be expressed as follows:

$$s = \frac{\rho}{|v|^{\frac{1}{\gamma}}}, \tag{10}$$

where s is the random step number, and $\gamma = 1.5$, $\lambda = 1 + \gamma$, ρ, and v obey a normal distribution:

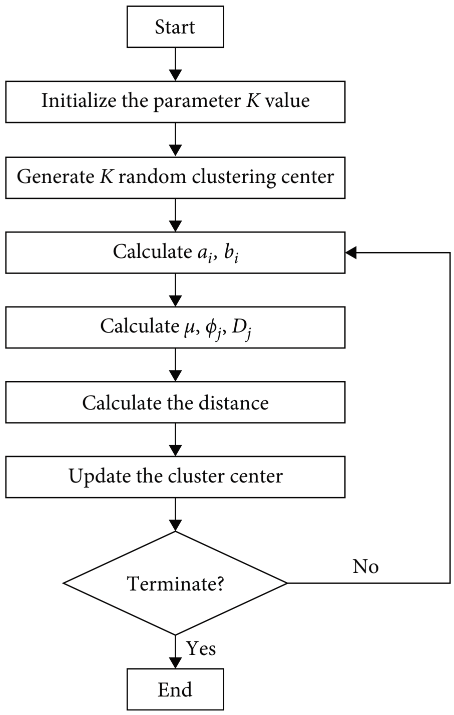

Figure 1: Flowchart of the LK-means algorithm.

$$\begin{cases} \sigma_\rho = \left[\dfrac{\Gamma(1+\gamma) + \sin(\pi \times \gamma/2)}{\Gamma\left((1+\gamma/2) \times \gamma \times 2^{(\gamma-1)/2}\right)} \right]. \\ \sigma_v = 1 \end{cases} \tag{11}$$

The Levy flight strategy can be generated based on the above equations.

A flowchart of the process of the LK-means algorithm is shown in Figure 1.

2.2. Determination of the Caving Zone and Fracture Zone Heights by Using the LK-Means Algorithm. To determine the caving zone and fracture zone heights, UDEC numerical simulations were conducted, and the block displacement was then obtained by using FISH language (secondary embedded language in the UDEC). Then, the LK-means algorithm was used to determine the fracture zone height and caving zone height. In our study, based on the displacement magnitude, the displacement data can be divided into two clusters, namely, a small displacement zone and a fracture zone, and the fracture zone can be further divided into two parts: a caving zone and another part of the fracture zone. It should be noted that the caving zone exhibits a larger displacement than the other part of the fracture zone. The determination process can be described as follows.

Step 1: The parameters of the LK-means algorithm are initialized. In this study, the upper rock mass of the goaf can be divided into two parts; hence, the *K* value is 2.

Step 2: Based on engineering practice, the UDEC numerical simulation model was constructed, and the block displacement was obtained by using the embedded FISH language in the UDEC.

Step 3: By using the LK-means algorithm, the upper rock mass of the goaf can be divided into two parts: a small displacement zone and a fracture zone. Based on the geometric parameters, the height of the fracture zone can be determined.

Step 4: Based on the above results, the fracture zone can be further divided into a caving zone and another part of the fracture zone by using the LK-means algorithm, and the height of the caving zone can then be determined.

Step 5: The process is terminated.

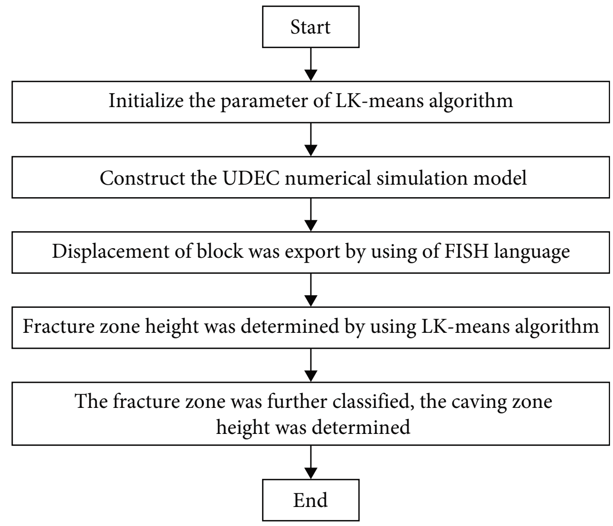

Figure 2: Flowchart of the determination of the caving zone height and fracture zone height.

The flowchart of the process for determining the caving zone height and fracture zone height is shown in Figure 2.

2.3. Example Verification of the Proposed Method. To verify the validity of the proposed method, an engineering practice example is given. A goaf exists in the Hongqing Coal Mine, which is located in Inner Mongolia in China, and the burial depth is 1,100 m. As shown in Figure 3, the size of the numerical simulation model is 196 m × 240 m, the width of the goaf is 100 m, the height of the goaf is 6.14 m, and the height of the model is 196 m. However, the buried depth is 1,100 m. Therefore, extra stress was loaded onto the top of the model, and the extra stress reached 22 MPa. In the numerical simulations, the Mohr–Coulomb model was used, and the corresponding mechanical parameters of the numerical simulations are listed in Table 1.

After the numerical simulations, a contour map of the displacement of the upper rock mass of the goaf can be obtained, as shown in Figure 4.

To determine the caving zone height and fracture zone height, the LK-means algorithm was utilized. To reduce the calculation time, the displacement at the center of the goaf was used. Based on the LK-means algorithm, the fracture zone height was determined, as shown in Figure 5.

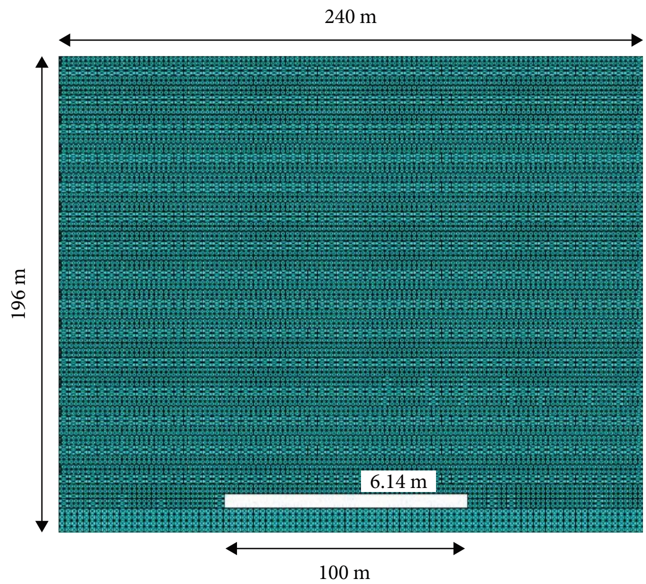

Figure 3: Geometry of the numerical simulation model.

Table 1: Mechanical parameters of the numerical simulation model.

Density (kg/m^3)	Bulk modulus (GPa)	Shear modulus (GPa)	Friction angle	Cohesion (MPa)	Tension (MPa)
2,426	12	7.2	35°	2	0.5

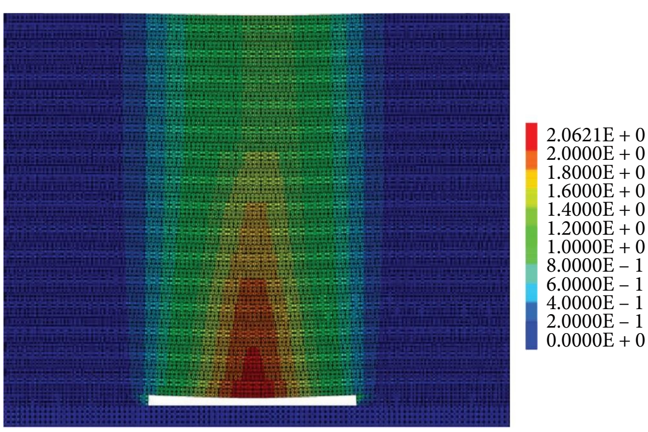

Figure 4: Contour map of the displacement (unit: m).

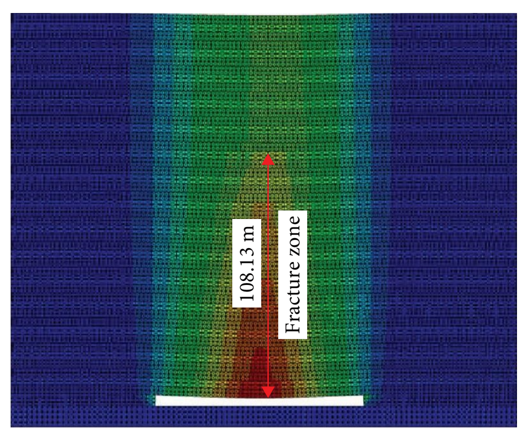

Figure 5: Determination of the fracture zone height.

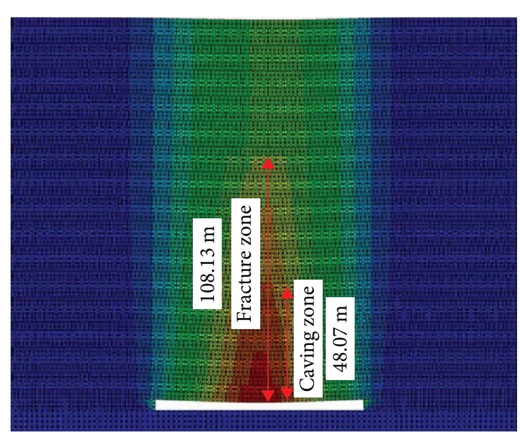

Figure 6: Determination of the caving zone height.

Because the fracture zone includes the caving zone, the fracture zone can be further divided into the caving zone and another part of the fracture zone based on the displacement magnitude, and the corresponding caving zone height can be obtained. The caving zone height is 48.07 m, as shown in Figure 6.

To validate the rationality of the proposed method, the caving zone height and fracture zone height were obtained. The caving zone height is 44.50 m, and the fracture zone height is 110.30 m, which are quite close to the numerical simulation results (the caving zone height is 48.07 m, and the fracture zone height is 108.13 m). The difference between the numerical simulation results and engineering test data is

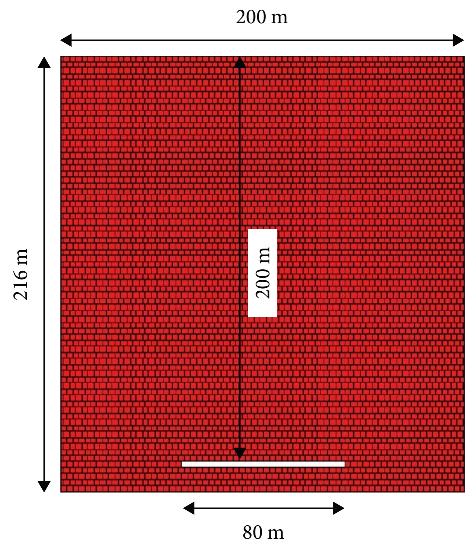

Figure 7: Numerical simulation model.

Table 2: Mechanical parameters of the numerical simulation model.

Density (kg/m^3)	Bulk modulus (GPa)	Shear modulus (GPa)	Friction angle	Cohesion (MPa)	Tension (MPa)
2,500	14.88	10.24	40°	11	2

small, and the error is acceptable, indicating that the proposed method is reliable.

2.4. Another Example. To further verify the validity of the proposed method, another example is given. In the Dongqu Coal Mine, the buried depth is 200 m, and the height of the working face is 3.19 m. The geometry of the UDEC numerical simulation model is shown in Figure 7.

The mechanical parameters of the numerical simulation model are listed in Table 2.

After the numerical simulation model was constructed, a contour map of the displacement magnitude was obtained, as shown in Figure 8, and the displacement magnitude was exported by using FISH language embedded in the UDEC. The exported data were used for determining the caving zone height and fracture zone height.

Based on the displacement magnitude and the LK-means algorithm, the fracture height and caving zone height were determined, as shown in Figure 9.

By using the LK-means algorithm, the fracture zone height and caving zone height were determined: the caving zone height was 13.17 m, and the fracture zone height was 43.31 m. In the field, the caving zone height and fracture zone height were measured: the caving zone height was 11.1 m, and the fracture zone height was 42.20 m. The fracture zone height and caving zone height calculated by using the LK-means algorithm are quite close to the measured values, indicating that the proposed method is reliable and can be applied in engineering practice.

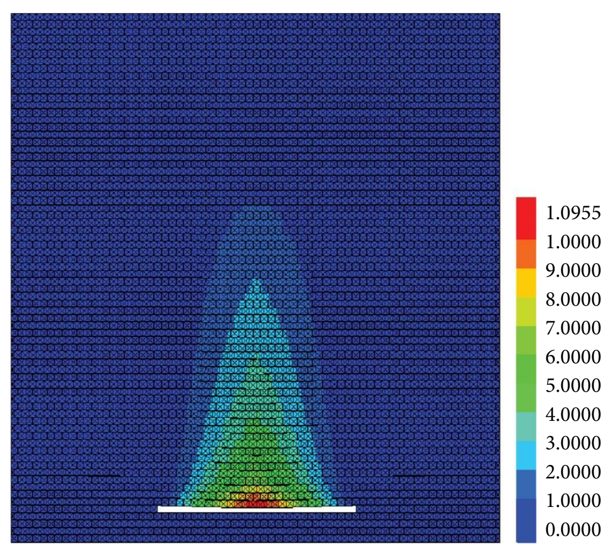

Figure 8: Contour of the displacement magnitude (unit: m).

3. Discussion

Caving zones and fracture zones frequently emerge when coal is excavated, and the caving zone height and fracture zone height are critically important for coal excavation design and gas drainage design. However, until now, there has been no empirical equation or method for estimating the caving zone height and fracture zone height.

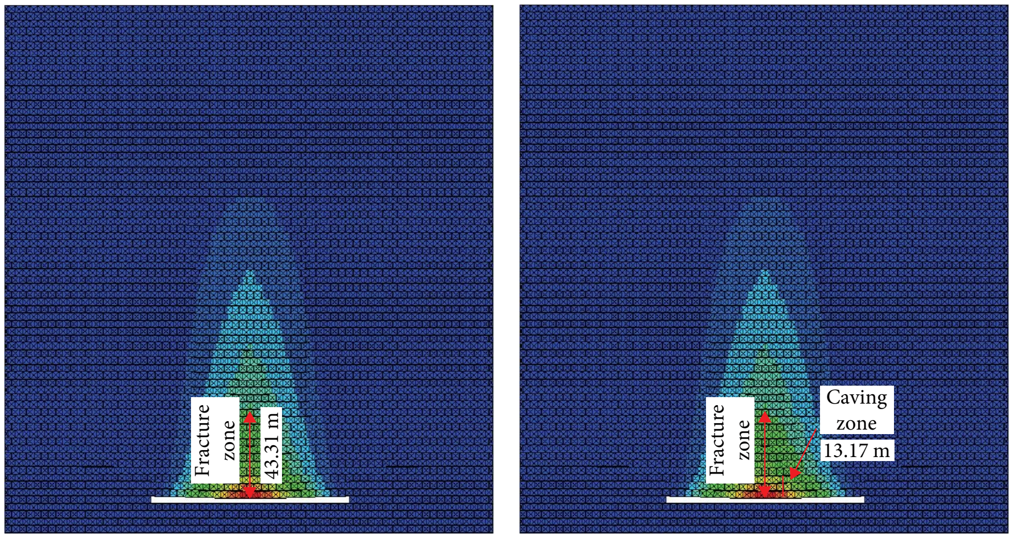

(a) (b)

Figure 9: (a) Fracture zone height and (b) caving zone height.

To resolve this problem, the UDEC numerical simulation method and LK-means algorithm were combined to determine the caving zone height and fracture zone height. The determination process is as follows: UDEC numerical simulations were first conducted. Thereafter, the simulated displacement magnitude was exported by using FISH language (embedded secondary language in the UDEC). The upper rock mass of the goaf was first divided into a fracture zone and a small displacement zone, and the fracture zone height was determined. Then, the fracture zone was divided into a caving zone and another part of the fracture zone, and finally, the caving zone height was determined. The classification method is based on the LK-means algorithm.

To verify the validity of the proposed method, two examples were given, and the corresponding caving zone height and fracture zone height were determined. Furthermore, the caving height and fracture zone height were measured in situ. By comparing the numerical simulation results and the in situ test data, the calculation results were quite close, indicating that the proposed method is reliable and can be applied in engineering practice.

However, many other factors may influence the fracture zone height and caving zone height, such as gas and underground water. These factors were not considered in our manuscript, which will be our next task.

4. Conclusions

To estimate the fracture zone height and caving zone height, UDEC numerical simulations were conducted. By using the LK-means algorithm, the caving zone height and fracture zone height were calculated, and the main conclusions of this paper can be summarized as follows:

(1) Based on engineering practice, the UDEC numerical simulation model was constructed, and numerical simulations were conducted. By using the LK-means algorithm, the upper rock mass of the goaf was divided into two parts: a fracture zone and a small displacement zone. Subsequently, the fracture zone was further divided into a caving zone and another part of the fracture zone. Then, the fracture zone height and caving zone height were determined.

(2) To verify the validity of the proposed method, two examples were given. The simulated fracture zone height and caving zone height were quite close to those obtained in engineering tests, which indicates that the proposed method is reliable. The proposed method can be applied to estimate the fracture zone height and caving zone height in engineering practice.

Data Availability

Data are available on request from the authors.

Conflicts of Interest

No potential conflicts of interest were reported by the authors.

Acknowledgments

This study was funded by the Guizhou Provincial Science and Technology Planning Project (Qian Science Strategy for Mining (2022)ZD001-05), the Guizhou Provincial Science and Technology Support Project (Qian Science Support (2021) Normal 347), the Guizhou Province General Higher Education Youth Science and Technology Talent Growth Project (Qian Education KY (2021) 258), and the Guizhou Institute of Technology High Level Talent Research Launch Fund Project (XJGC20190931).

References

[1] X. Meng, P. Zhao, X. Wang, L. Liu, and J. Yang, "Three zones, microseismic monitoring and analysis of gas drainage effect of overlying strata in gob of high dip gas seam," *Coal Science and Technology*, vol. 50, no. 1, pp. 177–185, 2022.

[2] J.-H. Wang, Z.-Z. Huang, and L. Yu, "Three piles in top coal, theory and its application in top caving mining for ultra-thick coal seams," *Journal of China Society*, vol. 42, no. 4, pp. 809–816, 2017.

[3] H. Ji, P. Xiang, F. Han, and Z. Yang, "Structural changes and failure mode of open-pit slope under underground mining disturbance," *Journal of China Coal Society*, vol. 37, no. 2, pp. 211–215, 2012.

[4] Y. Zhang, C. Liu, X. Zhang, K. Liu, S. Zhang, and G. Zhao, "The influence of ascending mining on the movement character of overlying coal seam in coal seams group," *Journal of China Coal Society*, vol. 36, no. 12, pp. 1990–1995, 2011.

[5] Z. Wang, J. Zhao, and Z. Li, "Determination of height of, three zone, in the stope with stagger position and internal misaligned roadway layout," *Journal of Mining & Safety Engineering*, vol. 30, no. 2, pp. 231–236, 2013.

[6] L. Zhou, X. Zhou, Y. Liang, and L. Wang, "Actual measurement analysis of three zones of goaf of 14308 working face with fully mechanized caving method of Dong tan Mine," *Journal of Liaoning Technical University*, vol. 25, pp. 52–54, 2006.

[7] Y. Fu, X. Song, and P. Xing, "Study of the mining height of caving zone in large mining height of caving zone in large mining height and super-long face of shallow seam," *Journal of Mining & Safety Engineering*, vol. 27, no. 2, pp. 190–194, 2010.

[8] X. Song, T. Gu, and Z. Yan, "Effects of increasing working faces length on underground pressure behaviors of mining super-high faces under shallow coal seam," *Chinese Journal of Rock Mechanics and Engineering*, vol. 26, pp. 4007–4013, 2007.

[9] Y. Teng, Z. Tang, and Z. Zheng, *The Research and Application of the Moving Law of the Ground Subsidence in Fully Mechanized Top Coal Caving*, China Coal Industry Publishing House, Beijing, 2009.

[10] J. Xu, X. Wang, and W. Liu, "Effects of primary key stratum location on height of water flowing fracture zone," *Chinese Journal of Rock Mechanics and Engineering*, vol. 28, no. 2, pp. 380–385, 2009.

[11] M.-S. Yi, W.-B. Zhu, L. Li, X. Zhao, and J.-L. Xu, "Water-inrush mechanism and prevention for fourth panel roof in Bulianta coalmine," *Journal of China Coal Society*, vol. 33, no. 3, pp. 241–245, 2008.

[12] J. Xu, W. Zhu, and X. Wang, "New method to predict the height of fracture water-conducting zone by location of key strata," *Journal of China Coal Society*, vol. 37, no. 5, pp. 762–769, 2012.

[13] M. Wang and P. Cao, "Numerical analysis of flattened Brazilian disc test based on the cusp catastrophe theory," *Mathematical Problems in Engineering*, vol. 2016, Article ID 4517360, 9 pages, 2016.

[14] M. Wang and P. Cao, "Calibrating micro-parameters of PFC2D(3D) model using the improved simulated annealing algorithm," *Mathematical Problems in Engineering*, vol. 2017, Article ID 6401835, 11 pages, 2017.

[15] Z. Tian, "Study on the distribution of, three zones, and overlying strata movement in the first mining face of Yuanzigou Mine," *Coal Mine Modernization*, vol. 5, no. 31, pp. 12–20, 2022.

[16] G. Guo, X. Zhang, and B. Zhang, "Detecting dynamic evolution law of roof fracture zone based on plugging leak test," *Coal Technology*, vol. 41, no. 8, pp. 150–153, 2022.

[17] Z. Liu, S. Zhang, and F. Huang, "Overburden migration law of inclined coal seam and determination of, upper three zones, height in Tengda Coal Mine," *Journal of Mining and Strata Control Engineering*, vol. 4, no. 3, Article ID 033028, 2022.

[18] P. Cui and X. Chen, "Study on height determination of, three zones, in goaf with large mining height working face," *Coal*, vol. 271, pp. 8–13, 2022.

[19] S. Chen, J. Bu, and B. Shi, "Quantitative study on, three zone, height of rock and mining fracture based on difference method," *Modern Mining*, vol. 632, pp. 149–152, 2021.

[20] S. Ren, "Numerical simulation study on height of water flowing fractured zone in Weiqiang Coal Mine," *Shangxi Coal*, vol. 40, pp. 11–16, 2021.

[21] K. Cui, "Research on height of, three zones, of overlying strata of working face with large mining height," *Energy and Energy Conservation*, vol. 11, pp. 24–27, 2021.

[22] H. Hu, J. Liu, X. Zhang, and M. Fang, "An effective and adaptable *K*-means algorithm for big data cluster analysis," *Pattern Recognition*, vol. 139, Article ID 109404, 2023.

[23] S. Dasgupta, N. Frost, M. Moshkovitz, and C. Rashtchian, "Explainable k-means and k-medians clustering," in *International Conference on Machine Learning*, pp. 7055–7065, PMLR, 2020.

[24] M. Ghadiri, S. Samadi, and S. Vempala, "Socially fair k-means clustering," in *Proceedings of the 2021 ACM Conference on Fairness, Accountability, and Transparency*, vol. 234, pp. 438–448, 2021.